A superstructure modulation induced by La doping of the layered manganate La$_x$Sr$_{4-x}$Mn$_3$O$_{10}$

H. Yang [a,b], Y.K. Tang [c], L.D. Yao [b], W. Zhang [b],
Q.A. Li [c], F.Y. Li [b], C.Q. Jin [b], R.C. Yu [b,*]

[a] *School of Science, Lanzhou University of Technology, Gansu Lanzhou 730050, PR China*
[b] *Laboratory for Extreme Condition Physics, Beijing National Laboratory for Condensed Matter Physics,
Institute of Physics, Chinese Academy of Sciences, P. O. Box 603, Beijing 100080, PR China*
[c] *State Key Laboratory of Magnetism, Beijing National Laboratory for Condensed Matter Physics,
Institute of Physics, Chinese Academy of Sciences, P. O. Box 603, Beijing 100080, PR China*

Abstract

In this paper, transmission electron microscopy (TEM) has been used for studying the slightly La-doped layered manganate La$_x$Sr$_{4-x}$Mn$_3$O$_{10}$. Albeit the samples for $x \leq 0.15$ appear single phased from the powder X-ray diffraction (XRD) analysis, the presence of numerous modulated domains in them has been revealed by electron diffraction and high-resolution electron microscopy. Electron diffraction data indicate that the local superstructure modulation is two-dimensional, and the modulation plane lies in the *ac* plane. The two primary modulation vectors are $\boldsymbol{q}_1 = (1/4)a^*$ and $\boldsymbol{q}_2 = (1/2)c^*$. High-resolution electron microscopy data suggest that the origin of the modulated structure is possibly attributable to an ordering of the La dopants. The locally modulated structure may have a correlation with the magnetic properties, typical of the ferromagnetic (FM) clusters, of the La$_x$Sr$_{4-x}$Mn$_3$O$_{10}$ manganate.
© 2006 Elsevier B.V. All rights reserved.

PACS: 75.47.Lx; 68.37.Lp; 91.60.Ed

Keywords: La$_x$Sr$_{4-x}$Mn$_3$O$_{10}$; TEM; Superstructure modulation

1. Introduction

The discovery of colossal magnetoresistance (CMR) in perovskite manganites (*R*, *A*)MnO$_3$ (*R* and *A* being trivalent rare-earth and divalent alkaline-earth ions, respectively) [1–3] has attracted considerable current interest in the study of physical and structural properties of the related system. Recently, a large amount of research activity has been performed on layered perovskite-related manganites with the general formula (*R*, *A*)$_{n+1}$Mn$_n$O$_{3n+1}$ aimed at understanding the influence of dimensionality on the magnetoresistance behavior. Structurally the (*R*, *A*)$_{n+1}$Mn$_n$O$_{3n+1}$ manganites have been shown to be able to crystallize in two kinds of layered structural type. One is representative of the Ruddlesden–Popper (RP) series [4] built up

from *n* layers of perovskite blocks alternating with single (*R*, *A*)O rock-salt layer. The other is generally called the hexagonal homologous series [5] which is based on such a building principle: blocks of *n* face-sharing [MnO$_6$] octahedra linked one to each other by two of the three terminal corners forming a two-dimensional sheet (as an example, Fig. 1 shows the [1 0 0] projection of the *n* = 3 structure of this series). However, from the structural point of view, the layered phases with even *n* members are missing from the latter series, but can be obtained with no limit to the members of *n* in the former one. For *n* = 1, both series reduce to a K$_2$NiF$_4$-type [6] layered structure with the (*R*, *A*)$_2$MnO$_4$ composition. When *n* = ∞, the (*R*, *A*)MnO$_3$ composition derived from the RP series forms three-dimensional perovskite structure, while that derived from the hexagonal series forms one-dimensional 2H structural type (e.g. BaMnO$_3$ [7]).

For the *n* = 3 member of the RP series, some detailed works were reported about Ca$_4$Mn$_3$O$_{10}$ [8–10]. However, attempts to

---

* Corresponding author. Tel.: +86 10 82649159; fax: +86 10 82649531.
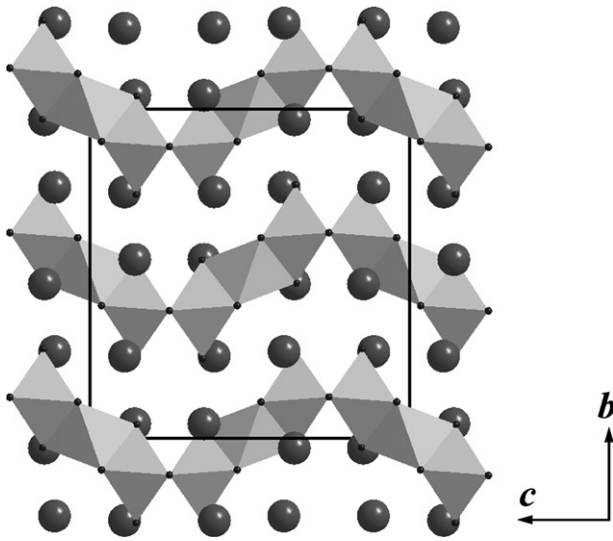*E-mail address:* rcyu@aphy.iphy.ac.cn (R.C. Yu).

Fig. 1. [1 0 0] projection of the $n = 3$ structure of the hexagonal layered manganates, such as $Sr_4Mn_3O_{10}$ and $Ba_4Mn_3O_{10}$.

prepare $Sr_4Mn_3O_{10}$ and $Ba_4Mn_3O_{10}$ resulted in an $n = 3$ phase of the hexagonal series [11,12]. The two manganates are isostructural to $Cs_4Ni_3F_{10}$ [13] and have the *Cmca* space group. Higher members of the hexagonal series, such as $Ba_6Mn_5O_{16}$ ($n = 5$) [14,15], have also been stabilized. These hexagonal layered manganates were revealed by the magnetic measurements to be antiferromagnetic (AFM) insulators [11,12,14–16]. Up to now, despite many studies of the layered manganates belonging to the hexagonal series, little work has been concerned with the effects of doping by rare-earth elements. In the present study, we have carried out investigations on structural and magnetic properties of the La-doped $La_xSr_{4−x}Mn_3O_{10}$. Single-phase samples were obtained for $x \leq 0.15$ based on the powder X-ray diffraction (XRD) data, and the magnetic measurements indicate that ferromagnetic (FM) clusters are induced in them due to the slight La doping [17]. Interestingly, albeit the slightly La-doped $La_xSr_{4−x}Mn_3O_{10}$ samples appear single phased from the XRD analysis, the presence of numerous modulated domains

possibly associated with La ordering has been revealed by transmission electron microscopy (TEM). The formation of the FM clusters may have a correlation with those domains. Our TEM results, which are reported in this paper, also drop a hint that caution should be used when interpreting the physical properties of doped perovskite manganates according to the diffraction-averaged structures observed.

2. Experimental

Using $SrCO_3$, $MnCO_3$, and La_2O_3 as starting materials, polycrystalline samples of $La_xSr_{4−x}Mn_3O_{10}$ ($x \leq 0.15$) were synthesized by the standard method of solid-state reaction in air. The detailed process of the sample preparation is described in ref. [17]. Thin foils for electron diffraction (ED) and high-resolution transmission electron microscopy (HRTEM) studies were prepared by crushing the bulk specimens in an agate mortar filled with alcohol, and then dispersing the fine fragments suspended in alcohol on Cu grids coated with holey carbon support films. A Tecnai F20 field-emission electron microscope, installed at Beijing Laboratory of Electron Microscopy, Beijing National Laboratory for Condensed Matter Physics, was used for the TEM studies. All the TEM experiments were carried out at an acceleration voltage of 200 keV.

3. Results and discussion

The fundamental structure of the $La_xSr_{4−x}Mn_3O_{10}$ ($x \leq 0.15$) samples were first characterized by selected area electron diffraction technique. Reflection conditions revealed from the resultant electron diffraction data are compatible with a space group of *Cmca*, in agreement with the space group of nondoped $Sr_4Mn_3O_{10}$ [11]. The ED patterns recorded along the [1 0 0] and [0 1 0] zone-axis directions of the $x = 0.15$ sample are given as example in Fig. 2. The camera length was calibrated using TlCl, and the lattice parameters were derived from the ED patterns as: $a = 0.55$ nm, $b = 1.25$ nm, and $c = 1.25$ nm, agreeing well with those refined from XRD data [17].

The presence of local superstructure modulation in the $La_xSr_{4−x}Mn_3O_{10}$ manganate is found to be a striking feature resulting from the doping of La. The electron diffraction evidence for the superstructure modulation is given by the appearance of additional spots in addition to the fundamental
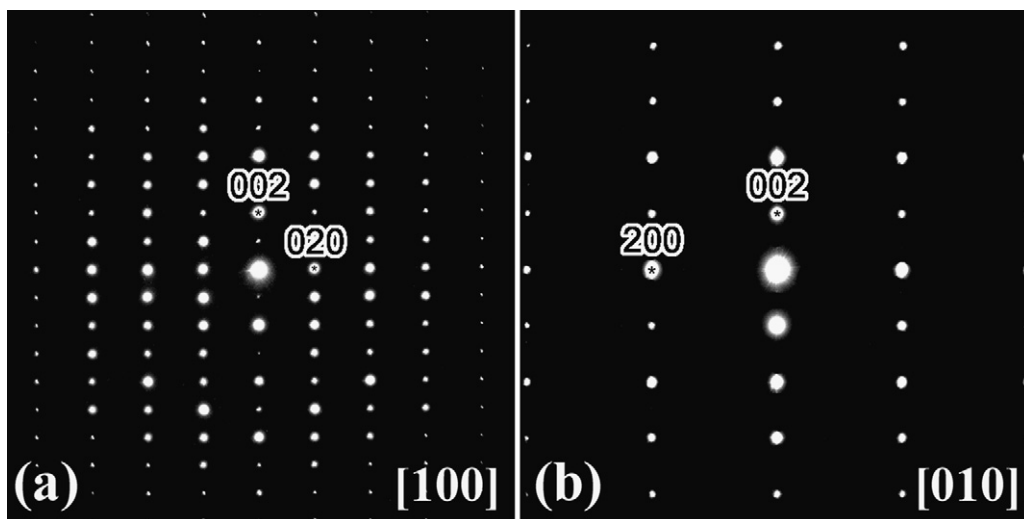

Fig. 2. ED patterns obtained from the perfect grains of $La_{0.15}Sr_{3.85}Mn_3O_{10}$ along (a) [1 0 0] and (b) [0 1 0].

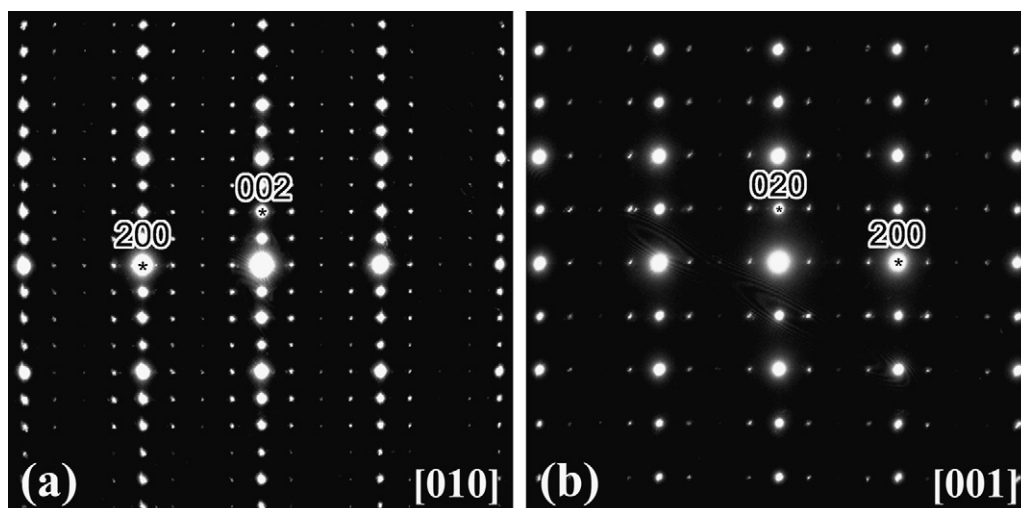Fig. 3. ED patterns collected on the modulated areas in the $La_{0.15}Sr_{3.85}Mn_3O_{10}$ sample along (a) [0 1 0] and (b) [0 0 1].

reflections in the ED patterns. Careful study of diffraction patterns along various orientations indicates that the structure modulation is two-dimensional, and the modulation plane lies in the *ac* plane. In the following work, we proceed to discuss the results obtained for the $x = 0.15$ sample. Figs. 3(a) and (b) present the ED patterns collected on the modulated areas in the [0 1 0] and [0 0 1] projections, respectively. Here we would point out that although the fundamental Bragg reflections in the [0 1 0] and [0 0 1] ED patterns construct similar tetragonal arrays, the two zone axes [0 1 0] and [0 0 1] can be easily differentiated from one another by convergent beam electron diffraction (CBED). From Fig. 3(a), one can see that commensurate (or nearly commensurate) superstructure reflections appear not only along the a^* direction with a four-fold periodicity of d_{200}, but also along the c^* direction with a two-fold periodicity of d_{002}. No trace of superstructure reflections is observed along the b^* direction as shown by the [0 0 1] ED pattern in Fig. 3(b), where the superstructure reflections with the four-fold periodicity of d_{200} are visible only along the a^* direction. These features are indicative of a two-dimensional characteristic of the superstructure modulation with the modulation plane lying in the *ac* plane. Therefore, the superstructure reflections can be characterized by two primary modulation vectors $q_1 = (1/4)a^*$ and $q_2 = (1/2)c^*$, and their systematic positions can be described as $((1/2)n, 0, m)$, where n and m are integers. In most cases, the ED patterns collected on the modulated areas present very weak superstructure reflections (an example is given in Fig. 4), indicating a short-range structure modulation in these areas. For a comparison we have also carried out TEM study on the nondoped $Sr_4Mn_3O_{10}$ sample. However, no trace of any modulated structure was detected, which consists with the previous results obtained from $Sr_4Mn_3O_{10}$ [11]. This fact suggests that the appearance of the superstructure modulation in the $La_{0.15}Sr_{3.85}Mn_3O_{10}$ manganate was caused obviously by the doping of La. Cation ordering (La/Sr) or charge ordering (Mn^{3+}/Mn^{4+}) are therefore considered to be the most possible factors resulting in the structure modulation.

In order to further reveal the origin of the structure modulation in the $La_{0.15}Sr_{3.85}Mn_3O_{10}$ phase, we turn to the HRTEM images. Fig. 5(a) shows a typical [0 1 0] HRTEM image of the modulated area. The fast Fourier transform (FFT) corresponding to the image is embedded on its top right-hand corner, indicating the typical characteristic of the two-dimensional superstructure modulation as described above. From this HRTEM image, one can see that the periodical distribution of the brightest spots, as indicated by the black arrows, is mainly attributed to the superstructure modulation. An intensity profile along the atomic layer outlined by white solid lines is shown in Fig. 5(b) and further reveals the modulation of the contrast. Further to discuss the origin of the modulation, it is necessary to properly correlate the spots with atoms in the image. It should be pointed out that this image was obtained under the defocus value of about -30 nm, which deviates from the Scherzer defocus (approximately -60 nm) [18]. The crystal thickness as estimated from the low-loss electron energy-loss spectroscopy (EELS)
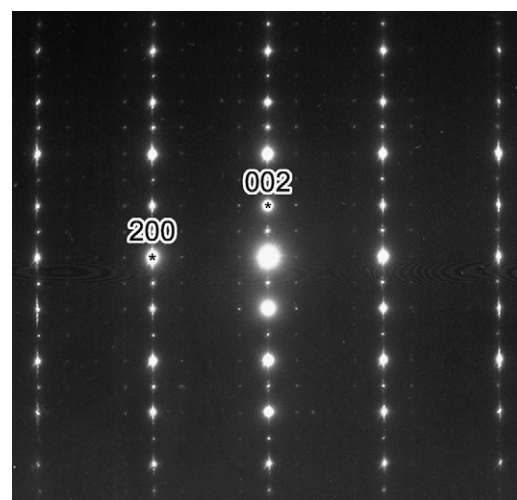

Fig. 4. ED pattern collected on the modulated area in the $La_{0.15}Sr_{3.85}Mn_3O_{10}$ sample along [0 1 0]. This ED pattern presents very weak superstructure reflections, indicating a short-range structure modulation in this area.
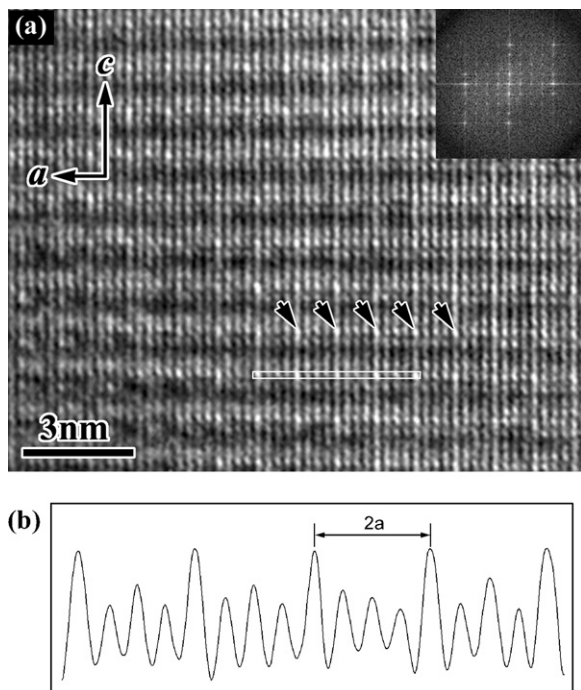
Fig. 5. (a) A typical [0 1 0] high-resolution TEM image of the modulated area in the $La_{0.15}Sr_{3.85}Mn_3O_{10}$ sample. The embedded is the corresponding FFT pattern of the image. From this image, one can see that the periodical distribution of the brightest spots, as indicated by the arrows, is mainly attributed to the superstructure modulation. (b) An intensity profile along the atomic layer outlined by solid lines, further revealing the modulation of the contrast.

spectrum was ∼5 nm. Under this circumstance, the projected rows of heavier atoms, such as La and Sr, appear as bright spots instead of dark ones. This was confirmed by image simulations based on the $Sr_4Mn_3O_{10}$ structure model [11] using multislice theory of dynamical scattering, whose results suggested that in a simulated image for the defocus value of −30 nm and the thickness of 4.9 nm, the Sr projected rows appear as bright spots. Based on this information, the brightest spots in the image (Fig. 5(a)) are reasonably considered as the La-containing rows, and the brighter ones represent the Sr rows. This suggests that the orderly distribution of the La dopants is possibly a key factor resulting in the superstructure modulation. To unambiguously determine whether the La ordering is indeed the main mechanism for generating the modulated structure, a detailed image simulation is required. Such a simulation is challenging because it is difficult to properly model the La ordering. In the absence of suitable simulation, the ordering of the La dopants can be only said to be a most possible factor leading to the formation of the modulated structure. The locally modulated structure revealed by our TEM may have a correlation with the formation of the FM clusters in the $La_xSr_{4-x}Mn_3O_{10}$ manganate [17].

4. Conclusions

By means of electron diffraction and HRTEM, the presence of numerous modulated domains in the slightly La-doped layered manganate $La_xSr_{4-x}Mn_3O_{10}$ has been revealed. The electron diffraction data indicate that the local superstructure modulation is two-dimensional, and the two primary modulation vectors are $q_1 = (1/4)a^*$ and $q_2 = (1/2)c^*$. The origin of the modulated superstructure is suggested to be possibly attributable to an ordering of the La dopants based on the HRTEM data. The magnetic properties, typical of the FM clusters, of the $La_xSr_{4-x}Mn_3O_{10}$ manganate may have a correlation with the locally modulated structure.

References

[1] R.M. Kusters, J. Singleton, D.A. Keen, R. McGreevy, W. Hayes, Physica B 155 (1989) 362.
[2] R. von Helmolt, J. Wecker, B. Holzapfel, L. Schultz, K. Samwer, Phys. Rev. Lett. 71 (1993) 2331.
[3] S. Jin, T.H. Tiefel, M. McCormack, R.A. Fastnacht, R. Ramesh, L.H. Chen, Science 364 (1994) 413.
[4] S.N. Ruddlesden, P. Popper, Acta Crystallogr. 11 (1958) 541.
[5] K. Boulahya, M. Parras, U. Amador, J.M. González-Calbet, Solid State Ionics 172 (2004) 543.
[6] R.W.G. Wyckoff, Crystal Structures, J. Wiley, New York, 1965.
[7] A. Hardy, Acta Crystallogr. 15 (1962) 179.
[8] P.D. Battle, M.A. Green, J. Lago, J.E. Millburn, M.J. Rosseinsky, J.F. Vente, Chem. Mater. 10 (1998) 658.
[9] J. Lago, P.D. Battle, M.J. Rosseinsky, J. Phys.: Condens. Matter 12 (2000) 2505.
[10] R.C. Yu, S.Y. Li, J.L. Zhu, F.Y. Li, Z. Zhang, C.Q. Jin, I.G. Voigt-Martin, J. Appl. Phys. 90 (2001) 6302.
[11] N. Floros, M. Hervieu, G. van Tendeloo, C. Michel, A. Maignan, B. Raveau, Solid State Sci. 2 (2000) 1.
[12] V.G. Zubkov, A.P. Tyutyunnik, I.F. Berger, V.I. Voronin, G.V. Bazuev, C.A. Moore, P.D. Battle, J. Solid State Chem. 167 (2002) 453.
[13] R. Schmidt, J. Pebler, D. Babel, Eur. J. Solid State Inorg. Chem. 29 (1992) 679.
[14] K. Boulahya, M. Parras, J.M. González-Calbet, J.L. Martinez, Chem. Mater. 14 (2002) 4006.
[15] H. Yang, R.F. Yang, Q.A. Li, F.Y. Li, C.Q. Jin, R.C. Yu, J. Phys. Chem. Solids 67 (2006) 2365.
[16] K. Boulahya, M. Parras, J.M. González-Calbet, U. Amador, J.L. Martinez, M.T. Fernaández-Díaz, Phys. Rev. B 69 (2004), 024418.
[17] Y.K. Tang, X. Ma, Z.Q. Kou, Y. Sun, N.L. Di, Z.H. Cheng, Q.A. Li, Phys. Rev. B 72 (2005) 132403.
[18] O. Scherzer, J. Appl. Phys. 20 (1949) 20.